

The use of Hi-Res TGA, TG-FTIR, HT-DRIFT and HT-XRD in the study of the decomposition of $\text{La}_2(\text{C}_2\text{O}_4)_3 \cdot 10\text{H}_2\text{O}$

G. Vanhoyland, R. Nouwen, M.K. Van Bael, J. Yperman, J. Mullens^{*}, L.C. Van Poucke

Laboratory of Inorganic and Physical Chemistry, IMO, Limburgs Universitair Centrum, B-3590 Diepenbeek, Belgium

Received 20 September 1999; accepted 16 February 2000

Abstract

Using a combination of various techniques, more intermediate products could be detected during the thermal decomposition of $\text{La}_2(\text{C}_2\text{O}_4)_3 \cdot 10\text{H}_2\text{O}$ than from conventional TGA measurements. In this way a more complete and detailed decomposition mechanism is proposed. Direct identification of the intermediate phases with HT-DRIFT revealed the presence of another oxycarbonate $\text{La}_2\text{O}(\text{CO}_3)_2$, while with Hi-Res TGA a thermally unstable intermediate $\text{La}_2(\text{CO}_3)_3$ was detected. All this information is consistent with the data obtained from TG-FTIR spectroscopic measurements. © 2000 Elsevier Science B.V. All rights reserved.

Keywords: Lanthanum oxalate; Thermal decomposition; HT-DRIFT; Hi-Res TGA; HT-XRD; TG-FTIR

1. Introduction

$\text{La}_2(\text{C}_2\text{O}_4)_3 \cdot 10\text{H}_2\text{O}$ was synthesised in a study to obtain a homogeneous LSCO (C=Co) precursor by the oxalate co-precipitation method. Although the decomposition of the oxalate has already been studied by conventional thermal analysis techniques [1–3], TG analysis suggested that more intermediate products were involved besides those reported $\text{La}_2(\text{C}_2\text{O}_4)_3$, $\text{La}_2\text{O}_2(\text{CO}_3)$ and La_2O_3 . In this study, the TGA apparatus was coupled to FTIR spectrometer in order to identify the evolved gases. However, in some cases it was favourable for also the intermediate solids to be identified directly. This was achieved by HT-DRIFT and HT-XRD. Moreover, since no well-defined plateaux were observed in the TG weight loss–

temperature plots, this indicates that overlapping decomposition reactions are involved. In order to resolve these reactions as much as possible a high-resolution variant of the normal TG was used.

2. Experimental

2.1. Methods and apparatus

Thermogravimetric measurements (in dry air and argon) were performed with TGA Model 951-2000 and Hi-Res TGA 2950, both from TA Instruments. The first unit was on-line coupled to a Bruker FTIR IFS 48 spectrometer in order to identify the evolved gases [4]. In all coupled experiments, a resolution of 8 cm^{-1} was selected for the MCT detector. The inert working conditions of all the TGA equipment were checked using copper oxalate as a standard [5]. DTA measurements were carried out by heating at

^{*} Corresponding author. Tel.: +32-11-26-83-08;
fax: +32-11-26-83-01.

E-mail address: jules.mullens@luc.ac.be (J. Mullens)

10°C min⁻¹ in dry air using a DTA 1600-2000 (TA Instruments).

X-ray diffraction experiments were performed using a Siemens D-5000 with 2θ values from 8 to 70°. The configuration for the high temperature experiments consisted of a Göbel mirror ($K_{\alpha 1+2}$, Huber), a high temperature device with a Pt rod (Anton Paar, HTK 10) and a position sensitive detector (Braun). The Pt rod also contribute to the diffraction pattern (peaks at 39.76, 46.24 and 67.45° 2θ) and could, therefore, be used as an internal standard in order to determine shifts due to temperature differences. Each measurement took about 5 min but was preceded by a 1 min delay. In the range from 320 to 650°C, a diffraction pattern was measured at 5°C intervals from 8 to 70° 2θ (0.0184° 2θ stepsize). Outside this range, temperatures were selected from the TG weight loss response. For indexing purposes, a Ge-monochromator ($K_{\alpha 1}$), standard sample holder and scintillation detector were used.

HT-DRIFT measurements were performed on a Bruker IFS 66 spectrometer equipped with a high temperature — high pressure chamber (Spectratech) with parabolic ZnSe windows. A DTGS detector was used, for which a resolution of 4 cm⁻¹ was selected. About 2% of $\text{La}_2(\text{C}_2\text{O}_4)_3 \cdot 10\text{H}_2\text{O}$ was mixed with KBr. This sample was continuously flushed with N₂. In accordance with the X-ray diffraction experiments, there was a 1 min delay after arriving at the desired

temperature. In the region of interest (290–680°C) every 10°C a FTIR spectrum was recorded. At lower temperatures, the stepsize was 50°C.

3. Preparation of lanthanum oxalate [6]

A 0.1 M aqueous solution of $\text{La}(\text{NO}_3)_3 \cdot 6\text{H}_2\text{O}$ (Acros) was mixed with a 1.0 M aqueous solution of $\text{H}_2\text{C}_2\text{O}_4 \cdot 2\text{H}_2\text{O}$ (Merck). The water contents of both starting materials were checked in advance with TGA. The mixing of both solutions was carried out in a computer-controlled way with two motor-driven burettes (Schott Geräte T100). In each step, 0.2 cm³ of each solution was added with continuous stirring, up to a final volume of 40 cm³. The white precipitate was filtered through a 0.45 μm Millipore filter and washed with de-ionised water. Finally, the powder was dried in air.

The quality of the powder was checked by X-ray diffraction. The observed peak positions were corrected by applying a correction curve for SRM 675 (NIST), used as an external standard. Since the diffraction pattern could be indexed with Treor97 [7] and Dicolv91 [8] as a monoclinic unit cell ($a=11.351 \text{ \AA}$, $b=9.589 \text{ \AA}$, $c=10.454 \text{ \AA}$ and $\beta=114.498^\circ$) with reasonable accuracy ($M_{20}=22$ and $F_{20}=49$ (0.012, 35)), the powder was considered to be as a single phase.

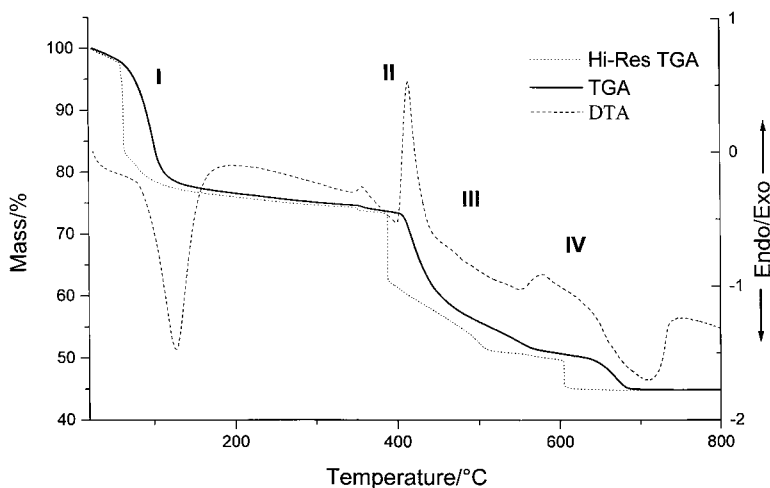


Fig. 1. DTA, normal and Hi-Res TGA of $\text{La}_2(\text{C}_2\text{O}_4)_3 \cdot 10\text{H}_2\text{O}$ in dry air.

Table 1
Comparison between calculated and observed weights from the Hi-Res TGA curve in dry air^a

Phase	Temperature (°C)	Observed weight (%)	Calculated weight (%)
La ₂ (C ₂ O ₄) ₃ ·3H ₂ O	72	82.1	82.0
La ₂ (C ₂ O ₄) ₃	347	74.4	74.5
La ₂ (CO ₃) ₃	390	62.6	63.0
La ₂ O ₂ (CO ₃)	556	50.7	50.9
La ₂ O ₃	601	44.8	44.8

^a All weights were calculated supposing that the last plateau corresponds with pure La₂O₃.

4. Results

4.1. TGA and DTA

In the normal mode, heating rate at 10°C min⁻¹, only the dehydration of the oxalate and the final decomposition from La₂O₂(CO₃) to La₂O₃ could be identified from the observed weight losses. The weight loss in the temperature range from about 300 to 700°C is clearly the result of overlapping decomposition reactions. Hi-Res TGA revealed which reactions were occurring (Fig. 1). The principle used was that when a reaction started, the heating rate was decrease in accordance to the mass loss. As a consequence, the temperatures at which the transitions occurred were better defined. Moreover, the experimental weight (62.6%) at the sharp curve transition around 390°C was in good correspondence with the calculated weight (63.0%) of La₂(CO₃)₃ (Table 1). Also in the

low temperature region, at least one different hydrated oxalate can be identified from a DTG analysis. Only at the temperature of about 350°C was the oxalate completely water free. From the observed decomposition curves in dry air and argon, it was apparent that the decomposition mechanism was not sensitive to the atmosphere. The rate of weight loss–temperature have the same shape, except for the fact that in argon the final decomposition reaction occurs at a somewhat elevated temperature. From DTA, it is clear that the decomposition of the ‘dry’ oxalate is highly exothermic. The consequence of this will be discussed later.

4.2. TG-FTIR

Experiments were performed both in dry air and argon atmosphere. The evolved gases were followed as a function of time (or temperature), and in both cases, four distinct regions could be distinguished

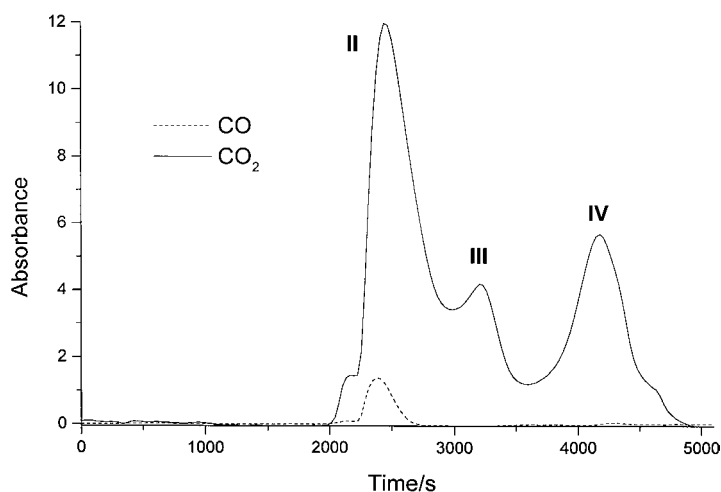


Fig. 2. Evolved CO and CO₂ as a function of time.

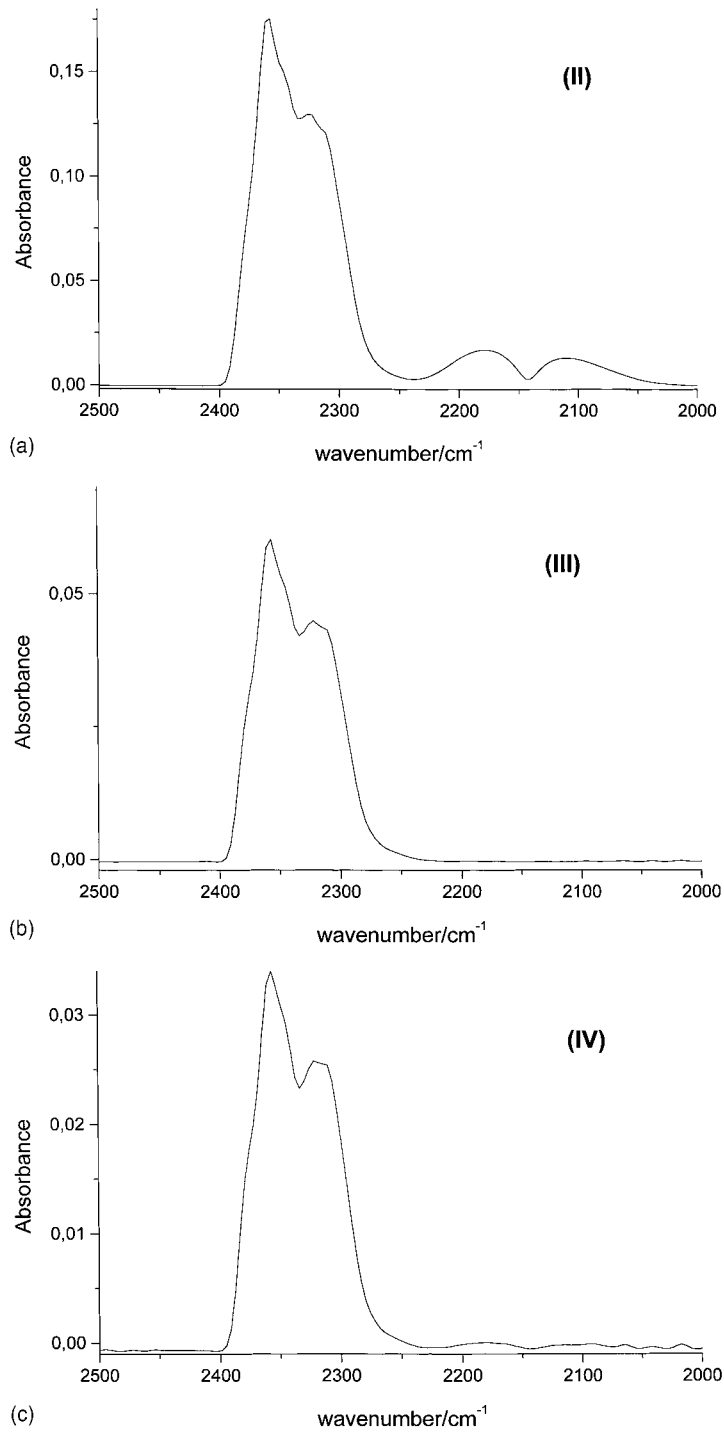


Fig. 3. Detailed IR spectra of: (a) region II; (b) region III; (c) region IV.

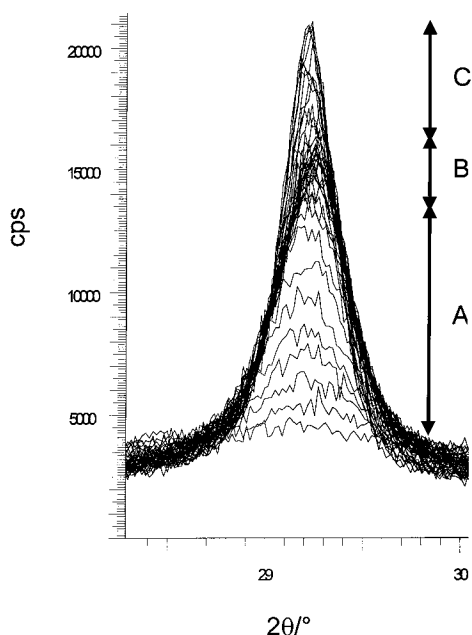


Fig. 4. Variation of the (1 0 3) diffraction peak of $\text{La}_2\text{O}_2(\text{CO}_3)$: (A) 425–470°C; (B) 470–570°C; (C) 570–630°C.

were gases were detected. In the first region (I), only water from the dehydration was detected. In all other regions (II, III, IV), CO_2 ($2400\text{--}2300\text{ cm}^{-1}$) absorbance could be detected. Furthermore, in the first part of region II, CO ($2200\text{--}2100\text{ cm}^{-1}$) was undoubtedly detected (Figs. 2 and 3).

4.3. HT-XRD

Up to about 60°C, there are only some minor modifications in the high angle region. Once this temperature is exceeded, the crystallinity decreased very fast and at about 100°C, the material was amorphous. No diffraction peaks were observed, but the background absorption level decreased, especially at low angles, until a temperature of about 425°C was reached. At this temperature, the first diffraction peaks of the $\text{La}_2\text{O}_2(\text{CO}_3)$ appeared and increased rapidly, but in the temperature range from 470 to 570°C, the intensity was almost constant. There was a further increase in peak intensity in combination with a small decrease in background level (Fig. 4). Finally, at 700°C, the diffraction peaks of La_2O_3 are observed.

4.4. HT-DRIFT

From these experiments, it was clear that the hydrated oxalate lost H_2O ($3600\text{--}3000\text{ cm}^{-1}$) up to about 270°C and in accordance with the TGA results, there was a large decrease in water around 100°C. Dehydration also changed the oxalate bands. Up to 100°C, they were situated at 1617, 1318 and 797 cm^{-1} [9] but from 150°C to the decomposition of the oxalate, they shift to 1638, 1307 and 784 cm^{-1} , respectively. Moreover, at 150°C, a small new band

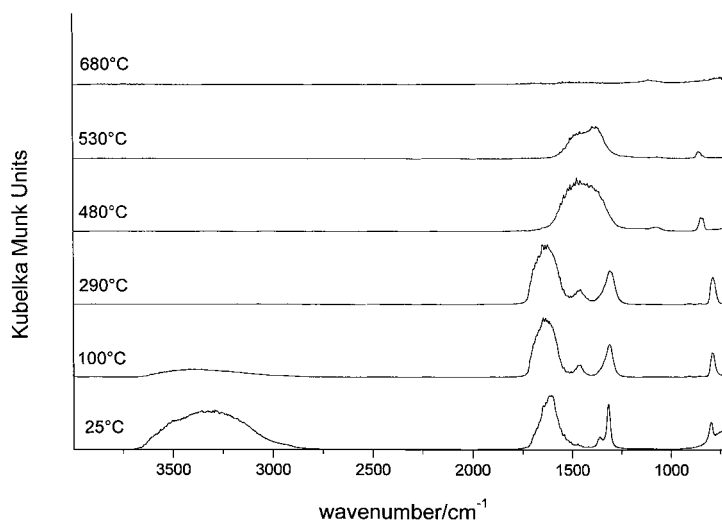


Fig. 5. HT-DRIFT spectra as a function of temperature.

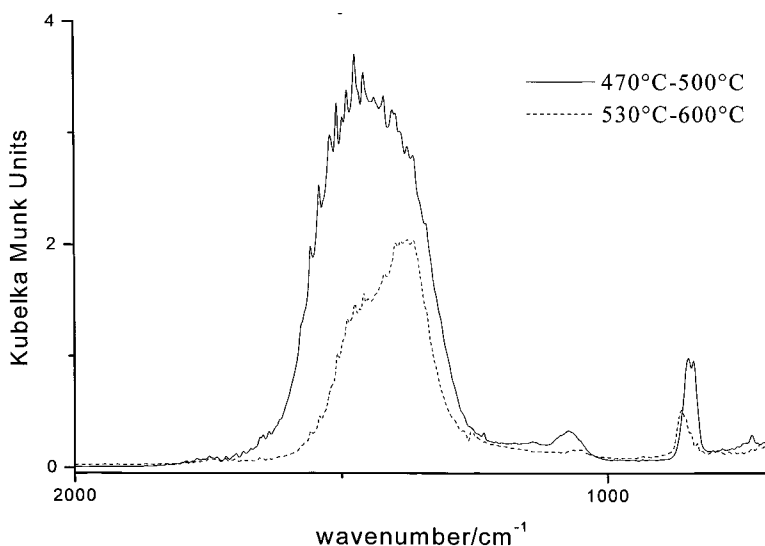


Fig. 6. Detailed IR of $\text{La}_2\text{O}(\text{CO}_3)_2$ (470–500°C) and $\text{La}_2\text{O}_2(\text{CO}_3)$ (530–600°C).

appeared at about 1460 cm^{-1} which increased slightly on heating. At 420°C , this band rapidly increased in absorbance and became broad at the expense of the oxalate bands, which have completely disappeared by 480°C . At the same time, new carbonate peaks appeared at 1074 cm^{-1} (weak) and 843 cm^{-1} (medium) [10]. Above 500°C , this phase decomposed into another, which remained stable up to $530\text{--}600^\circ\text{C}$. The bands of this new phase are at almost in the same positions as that of the previous phase before, except for broad band at 1460 cm^{-1} which shifts to 1379 cm^{-1} with a clear shoulder at 1460 cm^{-1} . Integrating from 1860 to 1175 cm^{-1} showed that the peak area was somewhat less than half that of the previous peak, suggesting that there are only half as much CO_3^{2-} groups present compared to the first phase. At 600°C , all peaks due to the CO_3^{2-} started to decrease and completely vanished at about 650°C (Figs. 5 and 6).

5. Discussion

From coupled TG-FTIR and HT-DRIIFT spectroscopies, it is clear that water is set free over quite a large temperature range. The highest mass reduction however, occurred below 100°C , consistent with $7\text{H}_2\text{O}$ molecules being removed. This suggests that

the H_2O molecules are present in different ways in the crystal structure.

The decomposition products $\text{La}_2(\text{C}_2\text{O}_4)_3$, $\text{La}_2\text{O}_2(\text{CO}_3)$ and La_2O_3 can be identified by mass calculation from the TGA and are confirmed by at least one other technique. For example, since $\text{La}_2(\text{C}_2\text{O}_4)_3$ is amorphous, XRD is not suitable but from the infrared absorption bands, the oxalate groups are clearly present.

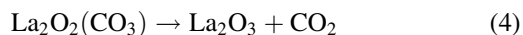
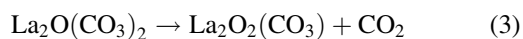
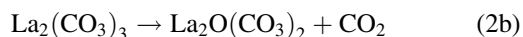
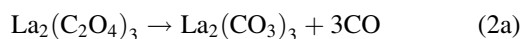
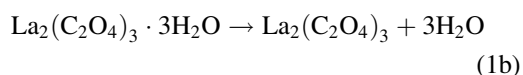
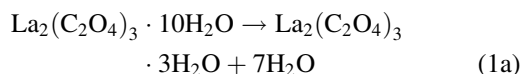
As mentioned before, a high resolution TGA reveals subtle differences in the weight loss–temperature curves than in normal mode, and it was apparent that the decomposition of the $\text{La}_2(\text{C}_2\text{O}_4)_3$ and $\text{La}_2\text{O}_2(\text{CO}_3)$ occurred in a two-step process. The real decomposition steps are both times preceded by a small decrease in mass that is observed over a restricted temperature area. The same effect is also seen with DTA and HT-DRIIFT. Concerning the decomposition of $\text{La}_2(\text{C}_2\text{O}_4)_3$ ($\pm 390^\circ\text{C}$), for example, the oxalate band around 1638 cm^{-1} is nearly constant while the stretching vibration of the carbonate group (1460 cm^{-1}) slightly increases in the temperature range $350\text{--}410^\circ\text{C}$. Once this last temperature is exceeded, there is a fast decrease in intensity of the oxalate bands, while for the carbonate bands the reverse is true.

Of all the techniques used, only Hi-Res TGA was capable, up to a certain level, to separate overlapping reactions. In this way, a thermally unstable intermedi-

ate phase such as $\text{La}_2(\text{CO}_3)_3$ could be identified. This was definitely not possible with HT-DRIFT and HT-XRD due to the discontinuous measuring regime. However, the existence of the $\text{La}_2(\text{CO}_3)_3$ as an intermediate phase is also suggested by the coupled TG-FTIR experiment, since in the whole experiment only once CO is evolved. This means that all the oxalate groups have to decompose to carbonate groups in one single step. In the coupled TG-FTIR experiment (continuous heating rate) CO_2 is detected at the same time due to the decomposition of the carbonate to an oxycarbonate, since both decomposition reactions are not enough resolved in time.

From the HT-DRIFT experiments, it's evident that in fact two different oxycarbonates must exist. First of all $\text{La}_2\text{O}_2(\text{CO}_3)$, which was also identified from HT-XRD, in the temperature range 530–600°C. However, from the curve integration, it follows that in the region 470–500°C, the $\text{La}_2\text{O}(\text{CO}_3)_2$ is uniquely present. In between, it's probably a mixture which exists.

These remarks in mind, we can summarise the whole decomposition mechanism:



However, since reactions 2a and 2b are highly exothermic, due to local heat build-up also reaction 3 can occur at the same time. In fact, this is clearly a mass effect and depending on the technique used. HT-XRD samples for example are about 50 times larger than those for HT-DRIFT and Hi-Res TGA. Moreover, in the HT-DRIFT set-up the sample is embedded in an inert material (KBr). This yields a more efficient heat removal compared to HT-XRD. For this reason $\text{La}_2\text{O}_2(\text{CO}_3)$ is partly formed when the oxalate decomposes in the HT-XRD experiment.

6. Conclusions

The decomposition mechanism of $\text{La}_2(\text{C}_2\text{O}_4)_3 \cdot 10\text{H}_2\text{O}$ is rather complicated by the fact that some decomposition reactions overlap with each other, so not all the intermediate products can be identified from the conventional TGA curve. Hi-Res TGA, however, has a much better resolving power. Moreover, the intermediate products can be identified in other ways: indirectly from the evolved gas analysis (TG-FTIR) or directly by other techniques as HT-DRIFT and HT-XRD. As has been showed in this case, combining all the information obtained from the different techniques is an efficient way in solving the puzzle.

Acknowledgements

G. Vanhoyland is research assistant of the Fund for Scientific Research, Flanders (Belgium) (F.W.O). M.K. Van Bael is postdoctoral fellow of the Fund for Scientific Research, Flanders (Belgium) (F.W.O.).

References

- [1] A. Górski, A.D. Krasnicka, *J. Therm. Anal.* 32 (1987) 1229–1241.
- [2] W. Ma-Shine, F. Tsang-Tse, *Mater. Chem. Phys.* 37 (1994) 278–283.
- [3] R.L.N. Sastry, S.R. Yoganarasimhan, P.N. Mehrotra, C.N.R. Rao, *J. Inorg. Nucl. Chem.* 28 (1966) 1165.
- [4] J. Mullens, in: M. Brown, P. Gallagher (Ed.), *Handbook of Thermal Analysis and Calorimetry*, Vol. 1, Elsevier, Amsterdam, 1998 p. 509.
- [5] J. Mullens, A. Vos, R. Carleer, J. Yperman, L.C. Van Poucke, *Thermochim. Acta* 207 (1992) 337.
- [6] A. Vos, R. Carleer, J. Mullens, J. Yperman, L.C. Van Poucke, *Eur. J. Solid State Inorg. Chem.* 28 (1991) 657–662.
- [7] P.E. Werner, L. Eriksson, M. Westdahl, *J. Appl. Cryst.* 18 (1985) 367–370, Treor97 is a further evolution of the well-known Treor90 indexing program.
- [8] A. Boulif, D. Louër, *J. Appl. Cryst.* 24 (1991) 987–993.
- [9] N.B. Colthup, L.H. Daly, S.E. Wiberley, in: *Introduction to Infrared and Raman Spectroscopy*, 3rd Edition, Academic Press, New York, 1990, p. 318.
- [10] N.B. Colthup, L.H. Daly, S.E. Wiberley, in: *Introduction to Infrared and Raman Spectroscopy*, 3rd Edition, Academic Press, New York, 1990, p. 310.